Research Square

Preprints are preliminary reports that have not undergone peer review.
They should not be considered conclusive, used to inform clinical practice,
or referenced by the media as validated information.

Blockage Mechanisms of Suspended Particles in Fractured Ultra-Low Permeability Reservoirs and Optimization of Water Quality Standards for Post-Fracturing Injection

Pei Li

lp5_cq@petrochina.com.cn

Oil and Gas Process Research Institute, PetroChina Changqing Oilfield Company

Peng Ren

Oil and Gas Process Research Institute, PetroChina Changqing Oilfield Company

Qianyi Mu

Oil and Gas Process Research Institute, PetroChina Changqing Oilfield Company

Zhanyou He

Oil and Gas Process Research Institute, PetroChina Changqing Oilfield Company

Zhixin Chen

Oil and Gas Process Research Institute, PetroChina Changqing Oilfield Company

Haoyun Li

Oil and Gas Process Research Institute, PetroChina Changqing Oilfield Company

Yan Li

Oil and Gas Process Research Institute, PetroChina Changqing Oilfield Company

Jihui Jiang

Oil and Gas Process Research Institute, PetroChina Changqing Oilfield Company

Feng Liu

Xi'an Shiyou University

Jin Luo

Xi'an Shiyou University

Article

Keywords: Ultra-low permeability reservoirs, Suspended particles, Suspended oil droplets, Blockage, Concentration Particle size

Posted Date: April 24th, 2026

DOI: https://doi.org/10.21203/rs.3.rs-9311405/v1

License: This work is licensed under a Creative Commons Attribution 4.0 International License.
Read Full License

Additional Declarations: No competing interests reported.

Abstract

The ecological and environmental management department requires the treatment of oilfield produced water to comply with the "Technical Requirements and Analysis Methods for Water Quality Indicators of Clastic Rock Reservoir Water Injection" SY/T 5329 – 2022. The water quality indicators of oilfield injected water (mainly suspended solids content, median suspended solids particle size, petroleum content, etc.) are strictly required, and the above water quality indicators are mainly determined based on the actual permeability of the reservoir. Hydraulic fracturing creates complex "pore-fracture" dual-media systems in ultra-low permeability reservoirs, but the blockage mechanisms of suspended solids during post-fracturing water injection remain unclear—rendering conventional homogeneous-media water quality standards inadequate. Using core samples and Brazilian splitting to simulate fractures, this study reveals distinct blockage behaviors of particles and oil droplets in fractured media. A critical particle-to-pore-throat diameter ratio (PC = 1.059) is identified to quantitatively distinguish internal pore blockage from external filter cake formation, bridging classical bridging theory with practical diagnosis. Fractures exhibit a dual effect: they mitigate overall permeability damage as preferential flow pathways, yet enable deep invasion of solids and oil, complicating subsequent removal. Orthogonal experiments with proppants demonstrate that stringent Class I standards can be relaxed to Class IV (particle size≤5μm, concentration≤25mg/L, oil content≤30mg/L) while maintaining permeability loss below 25%. By clarifying fracture-induced blockage mechanisms and validating relaxed standards, this study provides theoretical insights and practical guidance for cost-effective water injection in fractured ultra-low permeability reservoirs.

1. Introduction

Waterflooding is one of the primary methods for maintain reservoir pressure and maintaining stable production in low-permeability reservoirs[1, 2]. However, suspended solids present in the injected water—including suspended solid particles and emulsified oil droplets—can be captured by pore throats during seepage, causing physical blockage and an irreversible decline in permeability. This often results in increased injection pressure, injection-production imbalance, and reduced oil recovery[3, 4]. Therefore, controlling injected water quality is recognized as one of the core technical indicators in oilfield waterflooding development. The reservoirs in Changqing Oilfield have undergone hydraulic fracturing and long-term flushing with injected water, resulting in significant changes in actual permeability compared to the original permeability. Clarifying the variation law of permeability in low-permeability reservoirs under long-term water injection conditions is of great significance for determining the quality indicators of injected water in low-permeability reservoirs and reducing economic costs.

To better understand the relationship between water quality and formation damage, extensive core flooding experiments have been conducted worldwide. Early studies focused on unfractured matrix cores and revealed that particle blockage is governed by particle size, concentration, and their matching with pore throat dimensions. Barkman et al. [5] proposed the classic "1/3 to 1/7" bridging rule, suggesting that bridging plugging tends to occur when the ratio of particle diameter to throat diameter exceeds 1/3.

Gruesbeck et al. [6] demonstrated through experiments that there exists a critical velocity for particle migration and deposition. Below this critical velocity, particles primarily deposit at throats, forming blockages.

Subsequent studies on Chinese oilfields have further refined water quality criteria. For the Jianghan Oilfield, the optimal median particle size-to-throat diameter ratio was found to be ≤ 1/5[7]. In the Liaohe Oilfield, where the main throat diameter ranges from 10 to 27 μm, experimental results suggest that the particle size-to-throat diameter ratio should be between 1/2 and 1/3. For the Dagang Oilfield, recommended limits include oil content ≤ 15 mg/L, suspended particle size≤3μm, and suspended solids concentration ≤ 8 mg/L[8]. In the Changqing Oilfield, the reinjected water for the Ansai Oilfield must meet oil content ≤ 10 mg/L and suspended solids ≤ 2 mg/L [9, 10]. Luo Litao[11] et al. provided injection water quality recommendations for the Ansai Oilfield based on core flooding tests using actual rock samples: suspended particle concentration ≤ 2 mg/L, particle size < 4 μm; oil droplet concentration < 5 mg/L, droplet size ≤ 3.16 μm.

In addition to empirical criteria, mathematical models have been developed to describe permeability decline under different water qualities. Wang Jianzhong et al. [12] established mathematical models describing permeability decline under five different injection water qualities through numerous artificial core injection scouring experiments. Qin Lifeng[13] et al. analyzed the influence of key parameters—median particle size of suspended particles and throat radius—on permeability damage for injection waters with varying permeability levels in the western Weizhou Oilfield in the South China Sea. Tang et al. [14] identified suspended particles as the dominant damaging factor through displacement tests, while noting that clay mineral hydration swelling has negligible effects.

Collectively, these studies have significantly advanced the understanding of water quality-induced damage in unfractured reservoirs and provided a crucial foundation for the industry standard “Technical Requirements and Analytical Methods for Water Quality Indicators in Clastic Reservoir Water Injection” (SY/T 5329 – 2022). Based on this standard, environmental authorities currently enforce strict limits on suspended solids, median particle size, and oil content in produced water reinjection.

With the advancement of unconventional oil and gas development, ultra-low permeability reservoirs often require hydraulic fracturing to create artificial fracture networks for economic production. Fracturing fundamentally alters the reservoir flow regime, resulting in a dual-porosity and dual-permeability system. This transformation challenges conventional theories and water quality standards that are based on homogeneous porous media. Fractures may serve as preferential pathways for suspended particle transport, altering where and how blockages form. At the same time, proppant placement can modify fracture conductivity and particle retention behavior.

Currently, there is a lack of systematic understanding regarding the transport and blockage mechanisms of suspended particles in complex pore-fracture systems during post-fracturing water injection, as well as the resulting permeability evolution. Existing research and standards do not fully account for the

altered conditions following fracturing, leading to unnecessarily strict—and costly—wastewater treatment requirements in the field.

To address these gaps and support cost-effective water injection development in fractured ultra-low permeability reservoirs, this study focuses on the Ansai and Jiyuan Oilfields—both located in Northern Shaanxi with similar geological conditions but different microscopic pore-throat structures. Using actual core samples and the Brazilian splitting method to simulate hydraulic fractures, we systematically investigated flow behavior during water injection under various water quality conditions. The main objectives are: (1) to elucidate the blockage mechanisms of suspended particles and oil droplets in dual-porosity, dual-fracture media during post-fracturing water injection. (2) to quantify the impact of key water quality parameters—particle size, concentration, and oil content—on permeability damage. and (3) to evaluate the applicability of current water quality standards to fractured reservoirs and propose more practical, cost-effective control strategies. The findings are expected to guide the optimization of produced water reinjection processes and contribute to more efficient development of unconventional reservoirs.

2. Materials and Methods

2.1. Preparation of experimental materials

Laboratory instrumentation: mercury intrusion porosimeter, electronic balance, drying oven, ultrafiltration membrane, sand core filtration apparatus, digital high-speed stirrer. Based on the method established by Luolitau et al.[11], a colloidal suspension containing suspended particles and oil droplets was prepared via water-injection suspension techniques:

Suspended particle colloidal suspension: 5000-mesh quartz sand was selected as the suspended solid phase. The preparation steps are as follows (using a 1 μm particle size and 30 mg/L concentration as an example). The quartz sand was dissolved in simulated formation water and left undisturbed for 36 hours. The supernatant was then extracted and sequentially filtered through 0.9 μm and 1.1 μm membrane filters pre-soaked in simulated formation water using a filtration apparatus. The 0.9 μm filter membrane now retained quartz particles with sizes ranging from 0.9 μm to 1.1 μm. The average particle size of 1 μm was used as the size parameter. The membrane was dried at 25°C in a drying oven for 30 minutes, then weighed with a high-precision electronic balance (G_1). The same process was applied to a 0.9 μm filter membrane, recorded as G_2. The mass of particles adhered to the membrane was calculated as $m = G_1-G_2$. The membrane with the particles was repeatedly rinsed with simulated formation water, and the rinse solution was diluted to the desired concentration with simulated formation water.

Oil droplet suspension: diesel was used as the oil phase. The preparation involved: first, the inner wall of a beaker was repeatedly rinsed with a 0.1% cetyltrimethylammonium bromide (CTAB) surfactant solution, then dried to render the surface hydrophilic, minimizing oil droplet adhesion and concentration errors during formulation. One liter of simulated formation water was added to the beaker, along with

10.0 mg of diesel (chosen for its ease of droplet formation at room temperature and distinguishable color). The resulting oil-in-water suspension had a concentration of 10.0 mg/L. This suspension was stirred on a digital high-speed stirrer at 2000 rpm for 60 minutes.

Core samples were obtained from the Ansai and Jiyuan oil fields, representing the main productive strata. The natural cores were cut, dried, cleaned of oil, and fractured via Brazilian splitting to produce specimens 2–7 cm in length and approximately 2.5 cm in diameter, with or without hydraulic fractures (Fig. 1). The experimental saturated fluid mirrored the mineralization degree of the target reservoir's formation water, with $CaCl_2$-based simulated formation water (Ansai, 79.81 g/L; Jiyuan, 97.52 g/L).

2.2. Core flow evaluation experiment

Experimental methodology: Indoor core displacement tests adhere to the industry standard SY/T538-2010 "Reservoir Sensitivity Flow Evaluation Method."(Core fluid flow evaluation experiment apparatus is showed on Fig. 2) The specific procedures are as follows:

In accordance with the experimental design, injection fluids with varying water qualities were prepared by adding specified amounts of quartz sand particles or diesel droplets to simulated formation water. These prepared fluids were then injected into the core samples using the core flow evaluation apparatus. Core permeability was measured after every two pore volumes of injection. The displacement experiment was terminated after injecting 30 pore volumes of suspended particle solution or 10 pore volumes of suspended oil droplet solution. The degree of permeability damage caused by the injected water quality was calculated as the ratio of the permeability reduction to the initial permeability, where the permeability reduction is defined as the difference between the pre-blockage permeability and the post-blockage permeability. After the initial displacement, the core sample orientation was reversed, and a backflow plugging removal experiment was conducted using simulated formation water free of suspended solids. Permeability was measured again after this backflow procedure, and the permeability recovery factor was calculated to evaluate the effectiveness of the plugging removal. This recovery factor is defined as the difference between the permeability damage rate after plugging and the permeability loss rate after reverse unclogging. Finally, polynomial regression analysis was performed on all experimental data to evaluate the influence of key parameters—including suspended particle size, suspended particle concentration, and oil content—on the extent of permeability impairment in post-fracturing core samples.

3. Results and discussion

3.1. Microscopic pore throat analysis of low-permeability reservoirs

Core samples from An Sai and Ji Yuan oilfields were subjected to constant-speed mercury intrusion porosimetry (Fig. 3). The average pore throat radius in An Sai oilfield was measured at 0.472 μm, with an average pore radius of 140.174 μm, and an average pore throat network ratio of 355.89. In Ji Yuan

oilfield, the mean pore throat radius was 0.301 μm, the mean pore radius was 132.936 μm, and the pore throat network ratio was 462.23. The relatively large pore throat network ratio indicates that pore throat blockage by suspended particles significantly impacts the permeability of the core samples.

Based on the relevant research of the Ansai Oilfield and Jiyuan Oilfield [15–18], Porous medium characterized by high pore-throat coordination number, large pore-throat ratio, and multiple throats governing individual pores (Fig. 4).

3.2. The mechanism of suspended particles blockage

The average pore throat diameters of the Ansai and Jiyuan Oilfield core samples are 0.944 μm and 0.602 μm, respectively. Combining these with suspended particle sizes ranging from 0.15 μm to 1.8 μm, the particle-to-pore throat diameter ratio (PC) varies from 0.159 to 2.990 across the two oilfields. After injecting suspended particle solutions, all core samples exhibited positive permeability damage rates ($\alpha > 0$), confirming that particle invasion induces pore throat blockage and permeability reduction (Fig. 5). For a given PC value, α increases with higher suspended particle concentrations, indicating that particle concentration is a key factor controlling the extent of blockage.

Significantly, a critical transition in blockage behavior was observed at $PC \approx 1.059$. When $PC < 1.059$, α increases progressively with PC, suggesting that particles are small enough to enter the pore network and cause internal blockage by bridging or depositing within throats. This behavior is consistent with the classical bridging theory proposed by Barkman [5], which states that when the particle-to-throat ratio approaches unity, single-particle bridging becomes the dominant trapping mechanism. In contrast, when $PC > 1.059$, the rate of increase in α slows significantly for fractured cores and plateaus for unfractured cores. This indicates a shift from internal blockage to external filter cake formation, where particles are too large to enter the pores and instead accumulate at the core inlet face. This transition is a direct consequence of mechanical sieving, as particles larger than the pore throat cannot penetrate the porous medium.

Fractured cores consistently exhibited lower α values than their unfractured counterparts under identical PC conditions (Fig. 5). This can be attributed to fractures provide high-conductivity pathways that bypass the matrix pore network, allowing a significant portion of the suspended particles to flow through without being trapped. Similar observations have been reported by Lv et al. [19] in fracture–matrix core systems, where fractures acted as preferential channels, reducing overall permeability impairment. However, this does not imply that fractured cores are immune to damage; rather, the damage mechanism shifts from widespread matrix blockage to localized fracture-related entrapment.

The permeability recovery factor (β) after reverse flow cleaning provides further insight into the nature of the blockage (Fig. 6). For unfractured cores, β decreases with increasing PC when $PC < 0.710$, indicating that internal blockages formed in this regime are difficult to remove by backflow. This can be attributed to particles lodged within narrow throats are held by capillary and frictional forces that exceed the hydrodynamic drag during reverse flow. When PC exceeds 0.710, β increases, reflecting the transition to

external filter cake formation, which is more easily dislodged. For fractured cores, a higher critical PC of 1.113 was observed, and β was consistently lower than for unfractured cores across all PC ranges. This confirms that while fractures reduce the initial permeability damage, they create conditions for deep particle invasion and entrapment in complex fracture–matrix intersections, which are far more challenging to remediate.

The effluent particle concentration analysis (Fig. 7) supports this interpretation. For unfractured cores, when PC < 1.059, a fraction of particles exits the core, confirming that particles can traverse the pore network. Above PC = 1.059, effluent concentration drops to zero, indicating complete particle capture at the inlet face. For fractured cores, effluent concentration decreases gradually with PC and stabilizes at a non-zero value, reflecting continuous particle transport through fractures and partial retention within the fracture–matrix system.

These findings have important practical implications. In unfractured reservoirs, particles with PC < 1.059 cause internal damage that is difficult to remediate, whereas particles with PC > 1.059 form surface filter cakes that protect the interior but reduce injectivity. In fractured reservoirs, the same particles may penetrate deeply via fractures, causing internal damage that is both less severe initially but more persistent and harder to remove. This dual behavior underscores the need for fracture-specific water quality standards.

3.3. The mechanism of suspended oil droplet blockage

Suspended oil droplets exhibited fundamentally different blockage behavior compared to rigid particles. Permeability damage (α) increased monotonically with oil content for all core types, but the damage was consistently lower in fractured cores than in unfractured cores at the same oil concentration (Fig. 8). For unfractured cores, α exceeded 30% when oil content reached 10 mg/L, aligning with the Changqing Oilfield standard of ≤ 10 mg/L. This confirms that the existing standard is appropriate for matrix reservoirs.

The permeability recovery factor (β) after reverse flow cleaning was notably lower for fractured cores than for unfractured cores (Fig. 9). Moreover, β showed little variation with oil content, indicating that once oil droplets become trapped, their removal efficiency is not strongly dependent on concentration.

The contrasting behavior of oil droplets can be explained by their deformability and interfacial properties. Unlike rigid particles, oil droplets can squeeze through pore throats smaller than their own diameter under sufficient pressure, as governed by capillary forces [14]. Once inside the pore network, droplets may become trapped due to the Jamin effect—the additional capillary resistance generated when a deformable interface passes through a constriction. This trapping is exacerbated in fractured media, where droplets can enter deep into the formation via fractures and become lodged in matrix pores beyond the reach of reverse flow. Furthermore, oil droplets may coalesce, adsorb onto rock surfaces, or alter wettability, forming more stubborn blockages than particle-based filter cakes. These

mechanisms explain why oil-induced damage is more difficult to reverse in fractured reservoirs, despite being less severe initially.

In summary, while both suspended solids and oil droplets cause permeability damage, their mechanisms differ fundamentally. Particle damage is governed by size exclusion and concentration, with fractures offering partial protection but complicating remediation. Oil droplet damage is controlled by deformability, interfacial tension, and capillary trapping, with fractures enabling deep invasion and persistent blockage. These findings demonstrate that conventional water quality standards, developed primarily for unfractured reservoirs, are not directly transferable to fractured systems and require revision to balance cost and performance.

3.4. Orthogonal experiment on water quality for water injection

Embedding proppants within fractures significantly influences permeability sensitivity during water injection processes[20]. Currently, An Sai Oilfield and Ji Yuan Oilfield predominantly utilize 40–70 mesh ceramic proppants as stimulation agents[21, 22]. Applying the research methodology outlined by Hou Lei et al. [23] for artificially placing proppants in core samples post-fracturing. Referencing the experimental water quality standards from SY/T 5329 − 2022 for injection water in clastic reservoirs, orthogonal experiments were conducted with varying injection water qualities, recording core permeability loss rates under different conditions (Table 1). Post-fracturing permeability (K_s) markedly exceeds the initial permeability (K_0), indicating improved permeability due to fractures and proppants. Under optimal water quality conditions—classification I (suspended particle size D < 3μm, suspended particle concentration C_p<5mg/L, oil content C_o<8mg/L)—permeability loss was minimized at 11%. Conversely, under the poorest water quality—classification VIII (D < 5μm, C_p<25mg/L, oil content C_o<30mg/L)—permeability loss was maximized. According to SY/T 5329 − 2022, with initial core permeability K_0 ranging from 0.01×10^{-3} μm^2 to 0.5×10^{-3} μm^2, injection water should meet class II or III standards to satisfy water quality criteria. However, experimental results demonstrate that cores with fractures and proppants can still meet the ΔK < 25% permeability loss criterion even with class IV water quality.

Table 1 The results of the orthogonal experiments on water injection with different water qualities

Serial Number	Water quality grade	D	C_P	C_O	K_0	K_S	ΔK
		μm	mg/L	mg/L	10^{-3}μm^2	10^{-3}μm^2	%
1	□	3	5	8	0.0361	4.9242	11
2	□	5	15	10	0.0299	4.4583	16
3	□	5	20	15	0.0492	4.7081	18

Continued Table 1 The results of the orthogonal experiments on water injection with different water qualities

Serial Number	Water quality grade	D	C_P	C_O	K_0	K_S	ΔK
		μm	mg/L	mg/L	$10^{-3}μm^2$	$10^{-3}μm^2$	%
4	□	5	25	30	0.0518	4.0884	24
5	□	5	35	35	0.0328	4.3889	27
6	□	10	40	40	0.0398	3.9868	43
7	□	10	45	45	0.0248	5.1924	47
8	□	10	50	50	0.0682	4.1137	48

Therefore, all primary development blocks within the Changqing Oilfield, including Ansai and Jiyuan Oilfields, have undergone hydraulic fracturing stimulation. The current water injection quality standards are excessively stringent, leading to increased costs in wastewater treatment and consequently reducing the operational efficiency of the oil production facilities. Experimental results recommend that the hydraulically fractured sections of Ansai and Jiyuan Oilfields maintain suspended particulate sizes D<5μm, suspended particle concentrations C_p<25mg/L, and oil content C_o<30mg/L.

4. Conclusion

The goal of this paper is to provide a theoretical basis for the water quality of reservoir injection water in Changqing by studying how to obtain the actual permeability of reservoirs under long-term water injection after hydraulic fracturing transformation. This paper systematically investigated the blockage mechanisms of suspended solids in injected water on reservoir permeability after hydraulic fracturing in ultra-low permeability reservoirs. Using actual core samples from the Ansai and Jiyuan Oilfields and the Brazilian splitting method to simulate hydraulic fractures, a series of core flooding experiments were conducted to elucidate how suspended particles and oil droplets behave in the complex pore-fracture dual-media system. The findings address critical gaps in the understanding of post-fracturing water injection damage and provide a scientific basis for optimizing water quality standards. The main conclusions are as follows:

(1) The blocking behavior of suspended particles is jointly controlled by their particle size-to-throat diameter ratio (PC value) and concentration. When the PC value is low, particles can penetrate into the core, causing plugging; when high, particles predominantly form a filter cake on the outlet face, significantly reducing permeability but facilitating wellbore cleanup.

(2) The presence of artificial fractures significantly alters the plugging mechanism. Fractures provide preferential flow pathways, resulting in lower overall permeability decline in fractured cores compared to

unfractured cores. However, particles and oil droplets are more prone to enter deep pores along fractures, leading to internal plugging and more difficult subsequent cleanup.

(3) Suspended oil droplets, due to their deformability, can penetrate throat sizes smaller than their own diameter. Their plugging mechanism differs from that of solid particles. Higher oil content results in more severe permeability loss, and under fracture conditions, oil droplets are difficult to displace via reverse water injection.

(4) For reservoirs already undergoing hydraulic fracturing, there is potential to moderately relax current water quality standards for injected water. Under fracturing and proppant placement conditions, even when using Class IV water (suspended particle diameter ≤ 5 μm, concentration ≤ 25 mg/L, oil content ≤ 30 mg/L), core permeability loss remains below 25%, meeting development requirements. It is recommended to adjust water quality standards in fractured zones to reduce wastewater treatment costs and improve economic efficiency.

In summary, by establishing the first quantitative criterion (PC = 1.059) for distinguishing blockage types in fractured reservoirs and experimentally validating the feasibility of relaxing water quality standards, this study provides both a theoretical foundation and practical guidance for cost-effective water injection in ultra-low permeability reservoirs after hydraulic fracturing.

Abbreviations

The following abbreviations are used in this manuscript:

Symbol	Explanation
D_c	Diameter of the core channel
D	Particle size of suspended particles
PC	The ratio of the particle size of suspended particles to the diameter of the throat channel
C_p	Concentration of suspended particles
C_o	Oil content
K_0	Initial permeability of the core sample
K_p	Permeability after core splitting
α	Permeability loss rate
β	Permeability recovery rate

Declarations

Data Availability Statement

The raw data supporting the conclusions of this article will be made available by the authors on request.

Authorship contribution statement

Pei Li and Peng Ren: Conceptualization, Methodology, Writing – review & editing. Qianyi Mu. Zhanyou He and Zhixin Chen: Experimentation, Formal analysis, Writing – original draft. Haoyun Li: Supervision, Methodology. Yan Li: Investigation, Formal analysis, Visualization. Jihui Jiang: Visualization, Writing – review & editing. Feng Liu: Formal analysis, Investigation. Jin Luo: Experimentation, Writing – original draft.

Confidentiality Disclosure Statement

The authors declare that they have no known competing financial interests or personal relationships that could have appeared to influence the work reported in this paper.

Funding

This research was funded by the National Engineering Laboratory for Exploration and Development of Low-Permeability Oil and Gas Reservoirs (Grant Project: Research on the Permeability Variation Law during Water Injection Development in Low-Permeability Oil Reservoirs, Project Number: 2024-13312). The funding agency provided financial support for this research and did not participate in the specific research design, data collection and analysis, paper writing, or decision-making regarding publication.

References

1. Zou, M. & Li, X. Analysis of the Causes of Water Quality Changes in Oilfield Injection Water and Countermeasures for Stabilization [J]. *Chem. Eng. Manage. 2020* (29):191–192 .
2. Shi, G. et al. Influence of Injected Water Quality on Indigenous Microbial Flooding in Lu-9 Block of Xinjiang Oilfield [J]. *J. Nankai Univ. (Natural Sci. Edition) 2021*, **54**(04):101–107 .
3. Ye, Y. et al. The matching relationship between reservoir pore-throat structural parameters and suspended particle diameters [J]. *Petroleum Geol. Recovery Effi. 2009*, **16**(06):92–94 .
4. Yang, H. et al. Study on molecular aggregation mechanism of oilfield plugging based on molecular dynamics simulation [J]. *Appl. Chem. Ind.* **54** (10), 2566–2571 (2025).
5. Barkman, J. H. & Davidson, D. H. Measuring Water Quality and Predicting Well Impairment. *J. Petrol. Technol.* **24** (07), 865–873 (1972). SPE-3543-PA.
6. Gruesbeck, C. & Collins, R. E. Entrainment and Deposition of Fine Particles in Porous Media. *Soc. Petrol. Eng. J.* **22** (06), 847–856 (1982). SPE-8430-PA.
7. Hu, X. et al. Research on Water Quality and Management Technology of Injection Water in Jianghan Oilfield [J]. *J. Petroleum Nat. Gas Sci.*, (03):276–279. (2007).

8. Li, Y. et al. Research on the Quality Index System of Injection Water in the Coastal Area of Dagang Oilfield [J]. *Oil Gas Field Surf. Eng. 2012*, **31**(11):25–26 .
9. Yang, S. et al. Suggestions on the development of produced water reinjection in oil and gas fields in China in the new era [J]. *Nat. Gas Ind. 2022*, **42**(11):106–116 .
10. Wan, Y. On the Current Situation and Technological Development of Oilfield Produced Water Treatment and Re-injection [J]. Chemical Engineering Management,2019,(08):223 .
11. Luo, L. et al. Characteristic and Evolution Process of Fluid in Puguang Gas Reservoir[J]. *Geol. Sci. Technol. Inform.* **35** (01), 128–133 (2016).
12. Wang, J. et al. *Time-varying permeability of sandstone reservoirs under waterflooding of different water quality [J]* Vol. 42, 1234–1242 (Oil & Gas Geology, 2021). 05.
13. Qin, L. et al. Matching Relationship Between Suspended Particle Sizeand Reservoir Pore Structure in Water Injection Development[J]. *J. Xi'an Shiyou Univ. (Natural Sci. Edition)*. **39** (02), 47–54 (2024).
14. Tang, Y. M. et al. The mechanism of reservoir damage by water injection in ultra-low-permeability reservoirs and optimization of water quality index[J]. *Energies*, **18**(6) (2025). [2026-01-13].
15. Zhang, B. Study on microscopic pore throat structure of Chang 6 reservoir in Pingqiao area of Ansai oilfield [J]. *Petroleum Technol.* **31** (08), 230–232 (2024).
16. Chen, J. et al. Microstructure characteristics of Chang 6 tight sandstone reservoirs in Pingqiao area, Ansai oilfield, Ordos Basin [J]. *Petroleum Geol. Eng.* **36** (05), 35–40 (2022).
17. Han, J. et al. Characteristics of Micro-pore Structure and Differential Analysis of Logging Identification for Different Diagenetic Facies in Low Permeability Reservoir: A Case Study on Chang 61 Reservoir in Wangpanshan Area of Jiyuan Oilfield [J]. *Geoscience* **32** (06), 1182–1193 (2018).
18. Ren, D. et al. Formation Mechanism Of Chang 6tight Sandstone Reservoir. *Jiyuan Oilfield Ordos Basin[J] Earth Sci.* **41** (10), 1735–1744 (2016).
19. Lv, H. et al. Water-Injection Displacement Compatibility and Economic Performance in Fracture–Matrix Cores. *Acadlore Trans. Geosciences[J] 2025* **4**(1), 1–10 .
20. Zheng, L. et al. Stress sensitivity characteristics of tight sandstone of Xujiahe Formation in southern part of Sichuan Basin[J]. *Petroleum Geol. Recovery Effi.* **32** (06), 42–51 (2025).
21. Feng Ren, Han, J. et al. *Research and application of mixed water volume fracturing technology in tight reservoir, Ansai Oilfield [J]* Vol. 22, 530–533 (Fault-Block Oil & Gas Field, 2015). 04.
22. Li, C. et al. Research and Application of Oil Soluble & Water Viscous Fracturing Proppant [J]. Drilling & Production Technology,2021,44(01):65–68.
23. Hou, L. et al. Experimental Study on Permeability Evolution in Propped Shale Fracture[J]. *J. Southwest. Petroleum Univ. (Science Technol. Edition)*. **37** (03), 31–37 (2015).

Figures



Figure 1

Core samples of different fracturing fractures

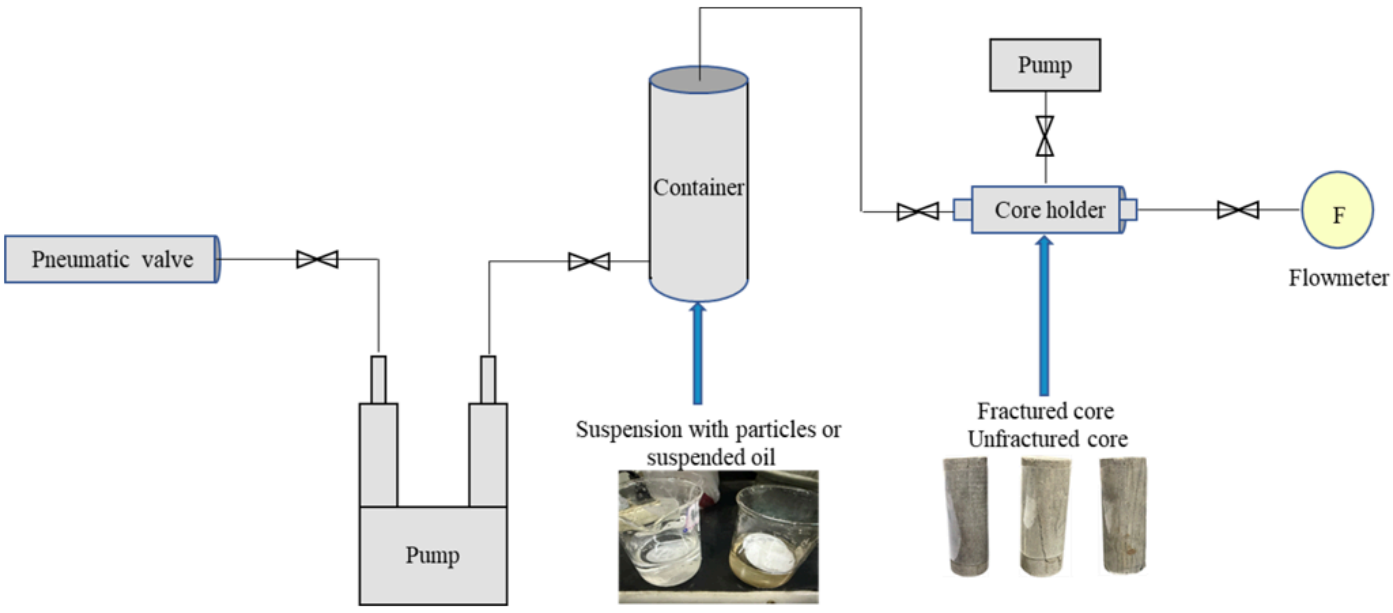


Figure 2

Core fluidity evaluation test apparatus

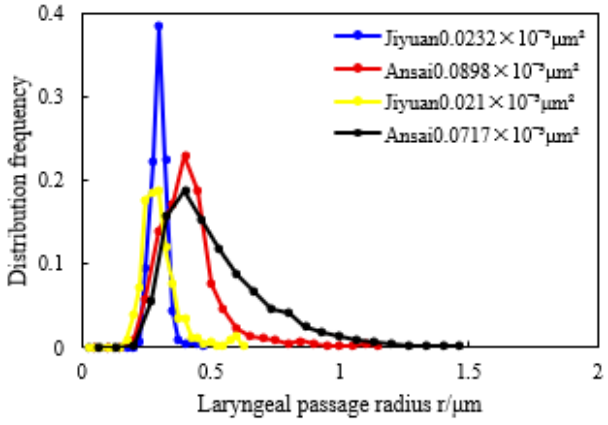


Figure 3(a)

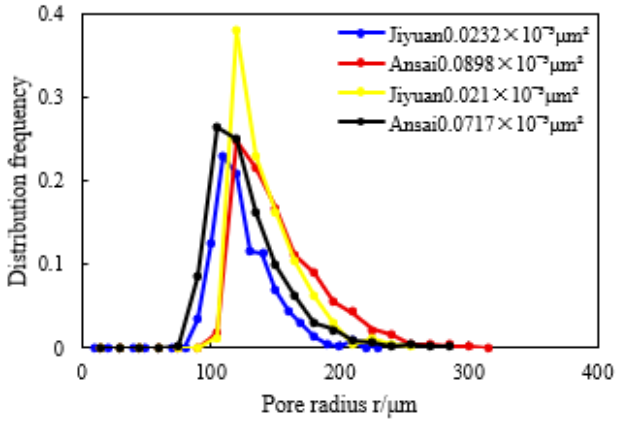


Figure 3(b)

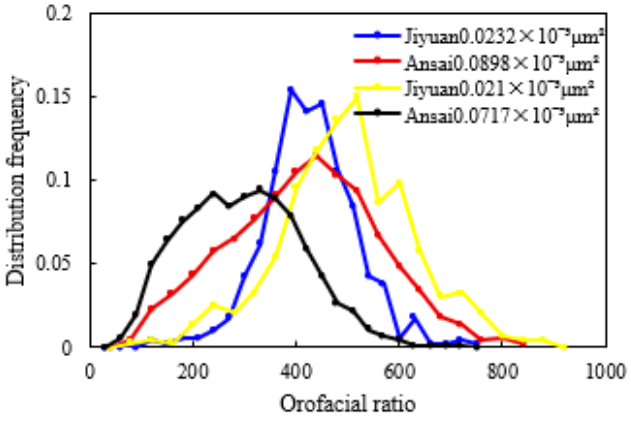


Figure 3(c)

Figure 3

(a) Distribution of core throat radius

(b) Distribution of core pore radius

(c) Distribution of the ratio of core pore throat radius

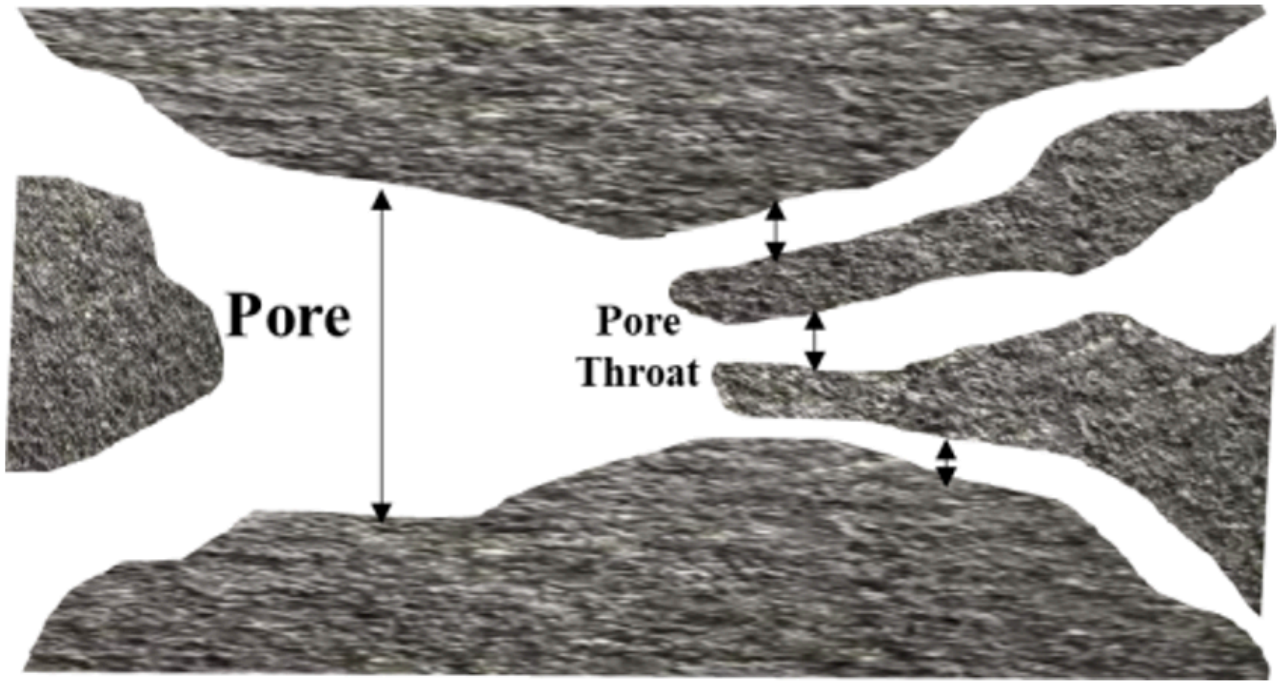


Figure 4

Diagram of pore-hole coordination relationship

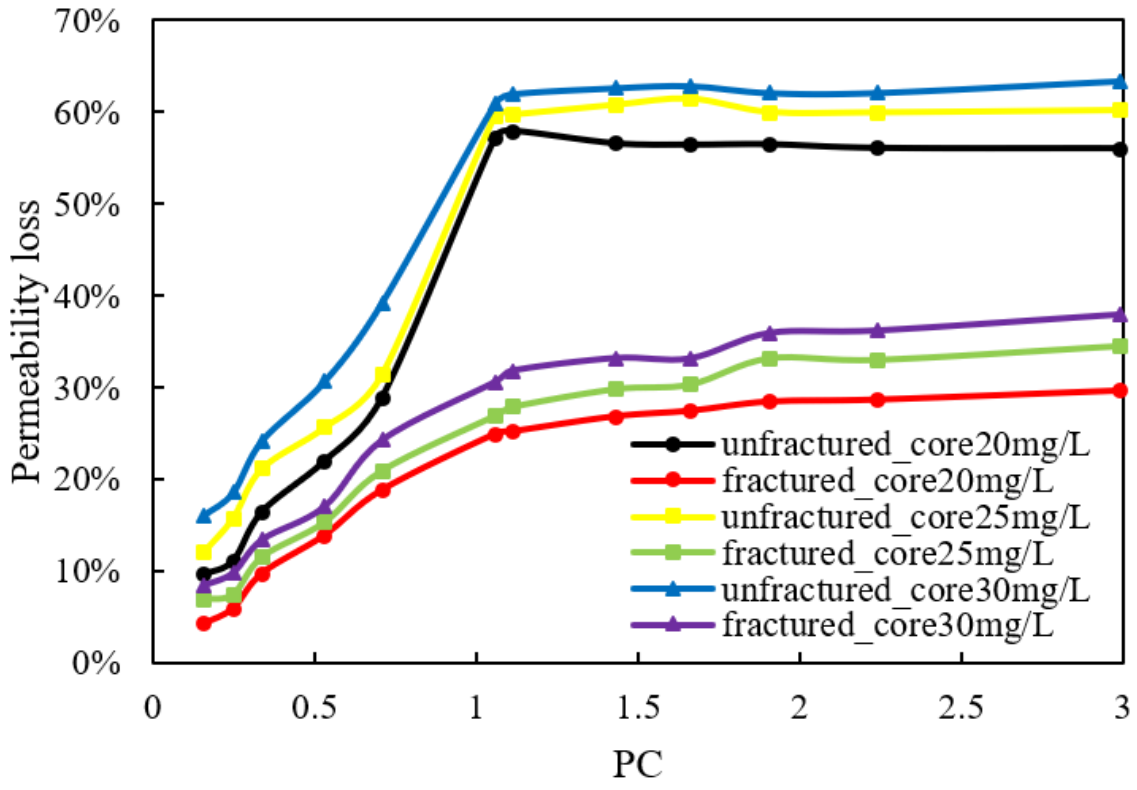


Figure 5

The relationship between the post-blockage permeability loss rate and PC

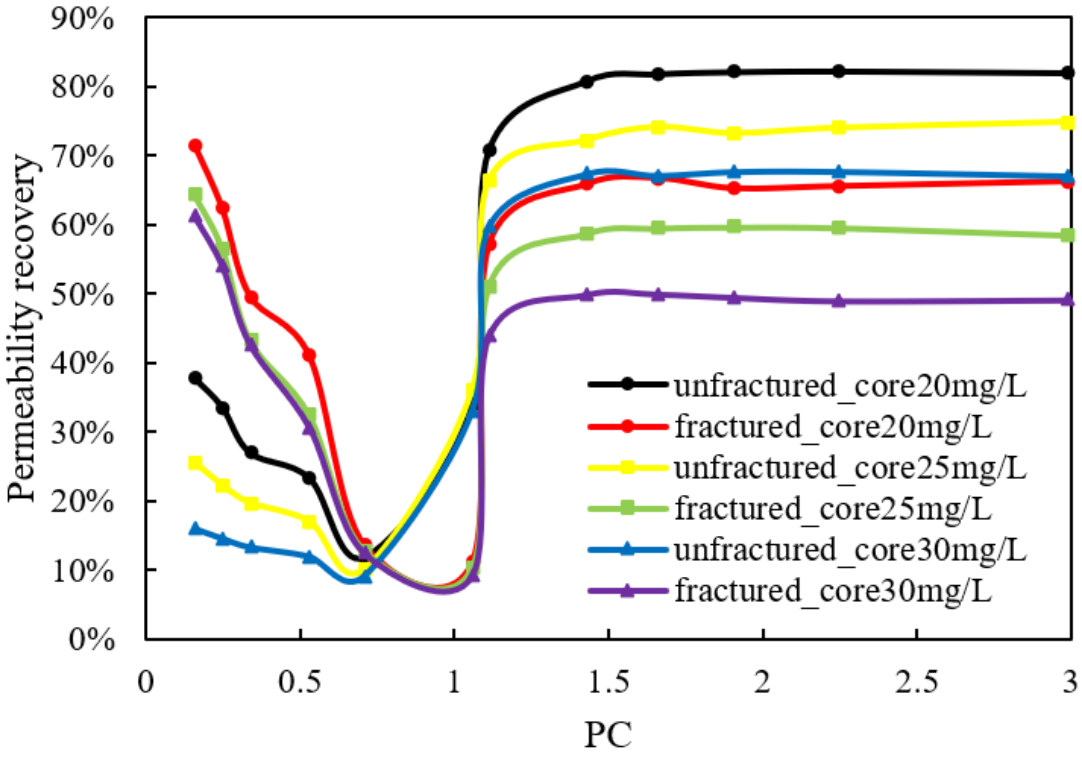


Figure 6

The relationship between the recovery rate of permeability after congestion relief and the PC

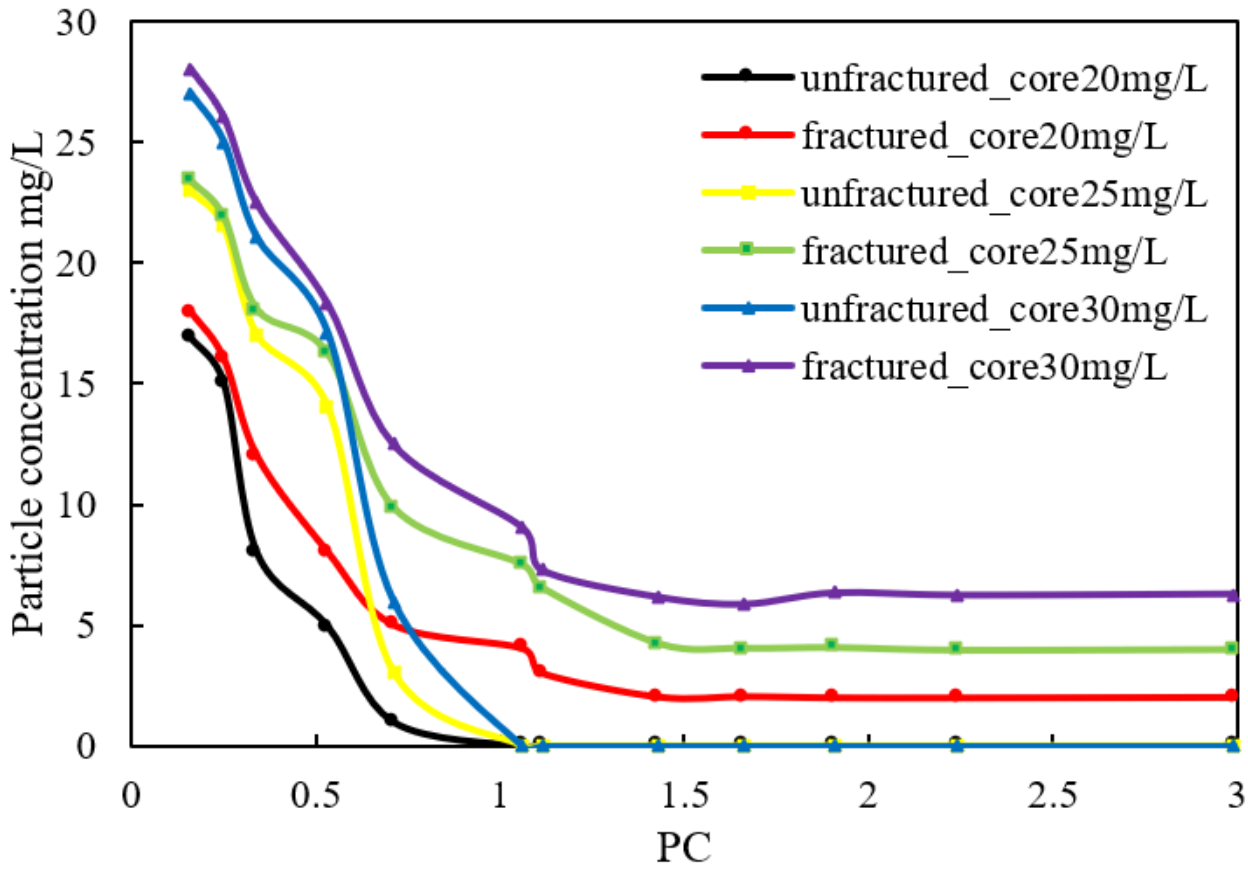


Figure 7

The relationship between the concentration of suspended particles in the effluent and PC

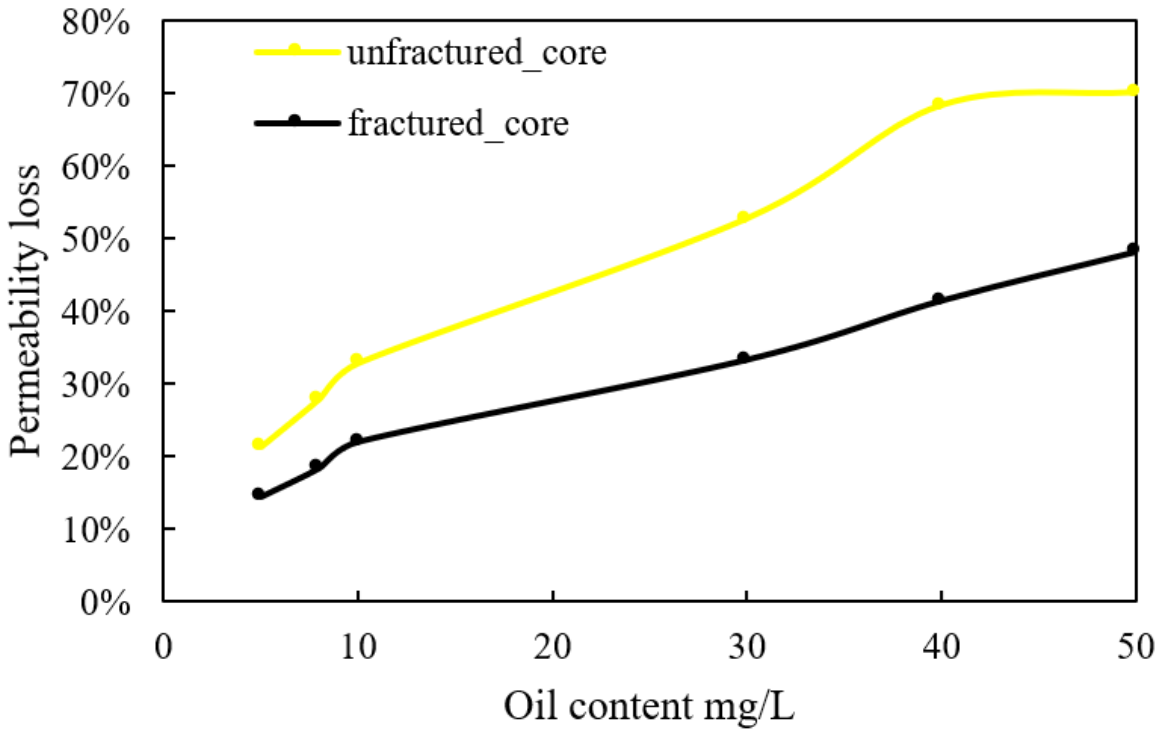


Figure 8

The relationship between the oil content of injected water and the loss rate of permeabilit

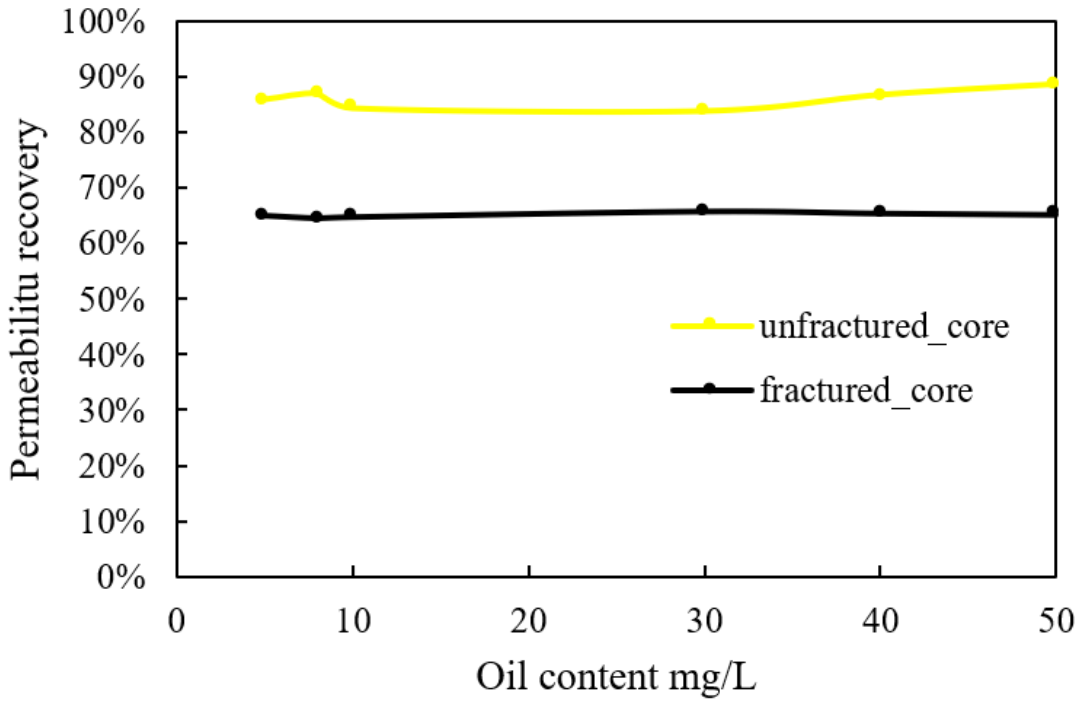


Figure 9

The relationship between the oil content of injected water and the recovery rate of permeability